Electronic Supplementary Material (ESI) for Nanoscale.

Electronic Supplementary Information

Functionalized Gold and Persistent Luminescence Nanoparticles Based Ratiometric Absorption and TR-FRET Nanoplatform for High-throughput Sequential Detection of L-cysteine and Insulin

Juan Li[a,b,c], Cheng Yang[c], Wen-Long Wang[c], Xiu-Ping Yan[a,b,c]*

[a] State Key Laboratory of Food Science and Technology, Jiangnan University, Wuxi 214122, China

[b] International Joint Laboratory on Food Safety, Jiangnan University, Wuxi 214122, China

[c] Institute of Analytical Food Safety, School of Food Science and Technology, Jiangnan University, Wuxi 214122, China

Table of Contents

Supplementary Notes

Insulin binding aptamer and it's complementary sequence:

Insulin binding aptamer (IBA):

5'-COOH-TTTTTTGGTGGTGGGGGGGGTTGGTAGGGTGTCTTC-3'

Partial complementary sequence 11 (CS):

5'-SH-C6-GAAGACACCCT-3'

Supplementary Figures S1-S18

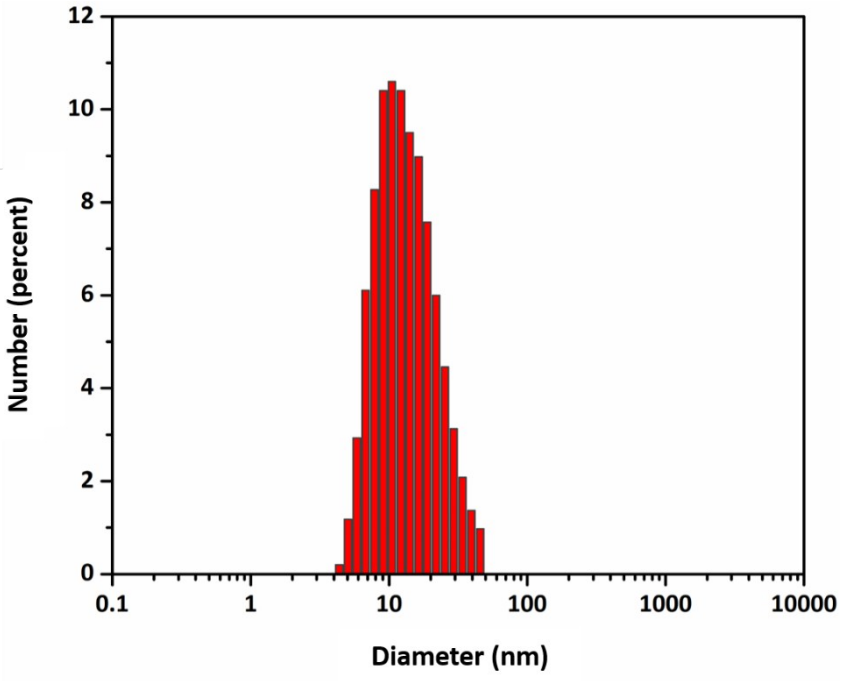

Figure S1. Size distribution by number of AuNPs.

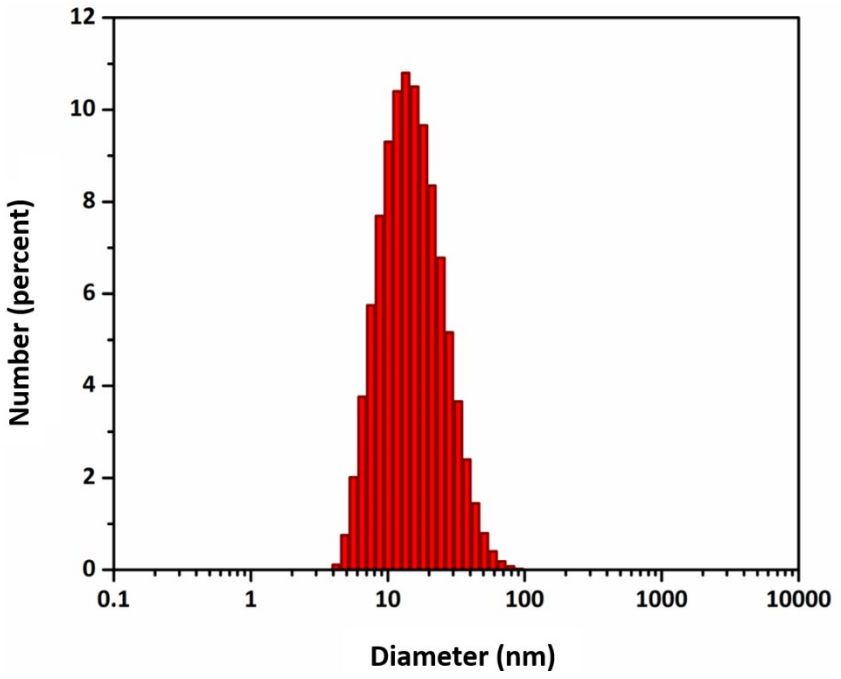

Figure S2. Size distribution by number of AuNP-CS.

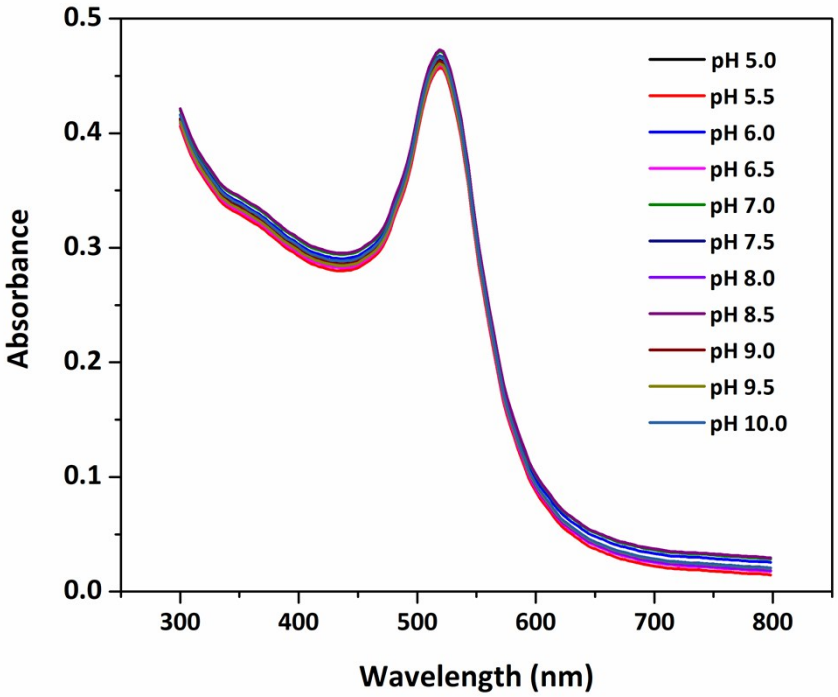

Figure S3. Effect of pH on the UV-visible absorption spectra of AuNP-CS.

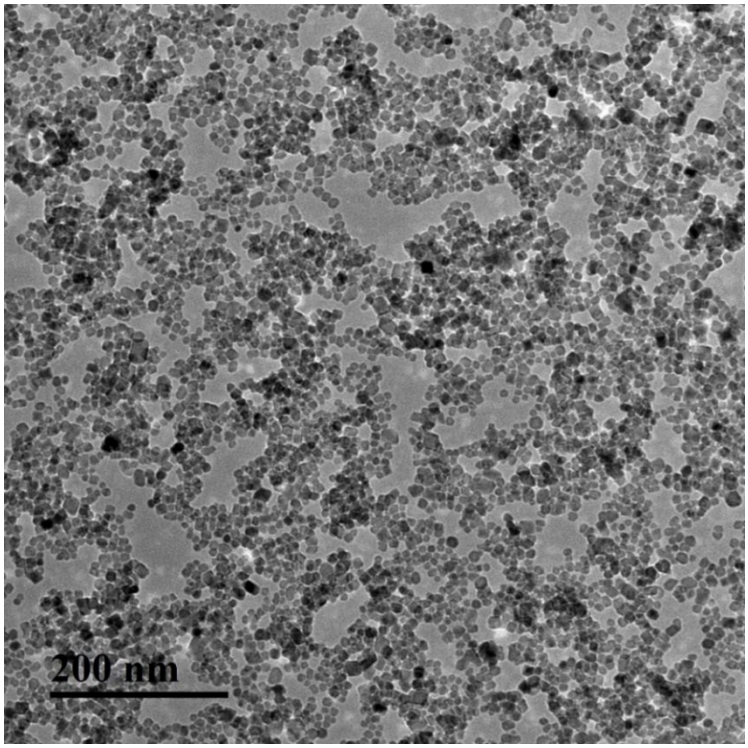

Figure S4. TEM images of the as-prepared PLNPs.

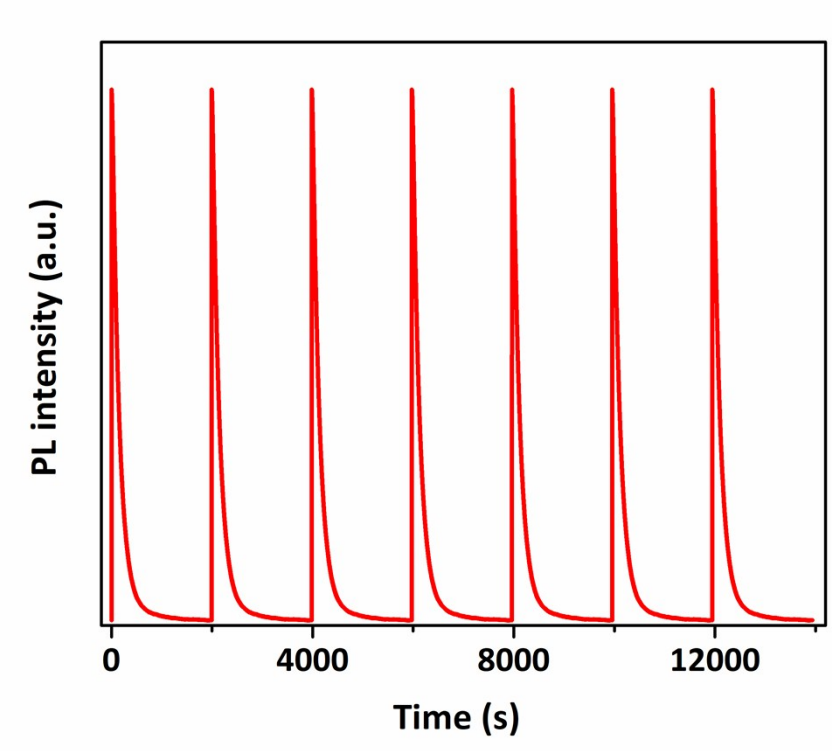

Figure S5. Afterglow decay curves (seven cycles) of the synthesized PLNPs by monitoring the Cr^{3+} emission at 698 nm upon 254 nm excitation.

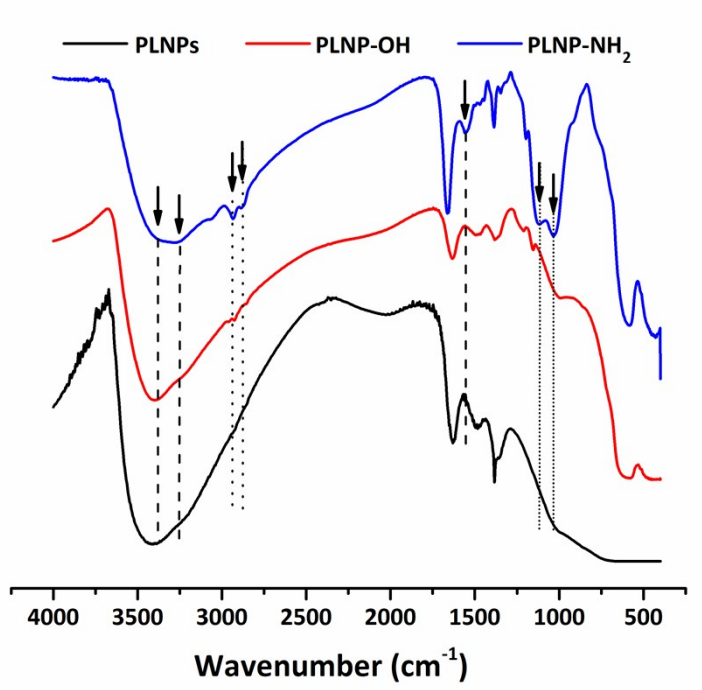

Figure S6. FTIR spectra of the bare PLNPs and functionalized PLNPs.

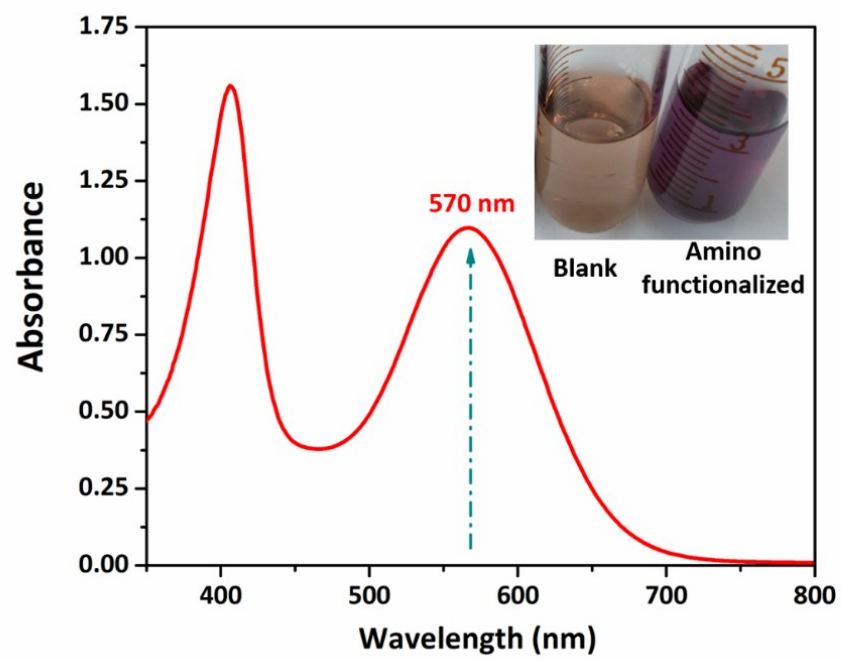

Figure S7. Absorption spectrum and photograph of ninhydrin test for the PLNP-NH_2.

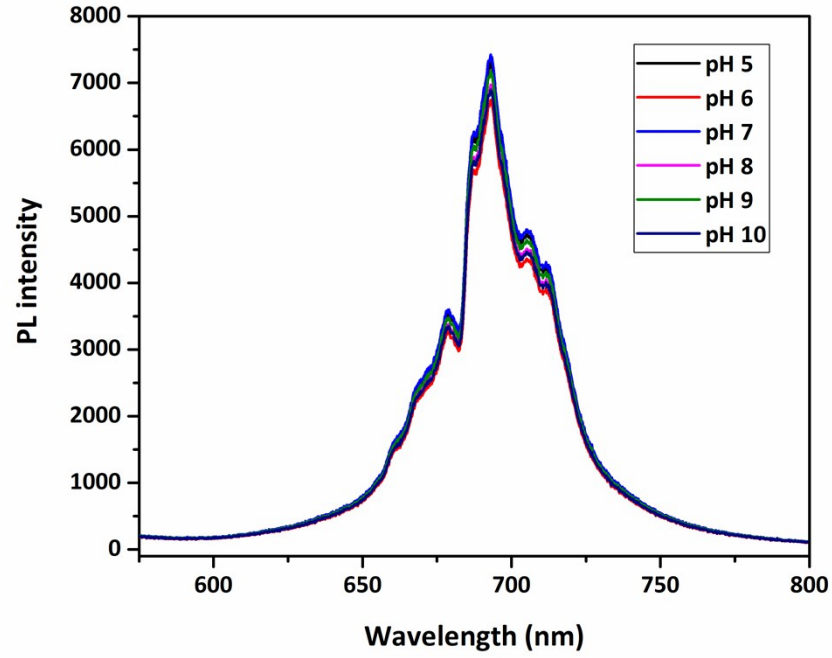

Figure S8. Effect of pH on the PL spectra of PLNP-IBA.

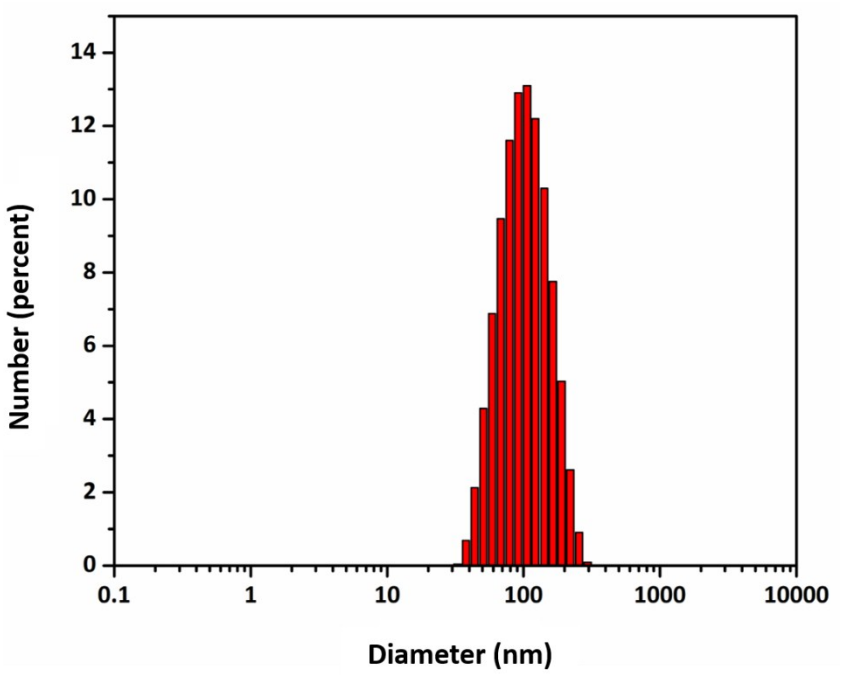

Figure S9. Size distribution by number of the L-Cys-AuNP-CS.

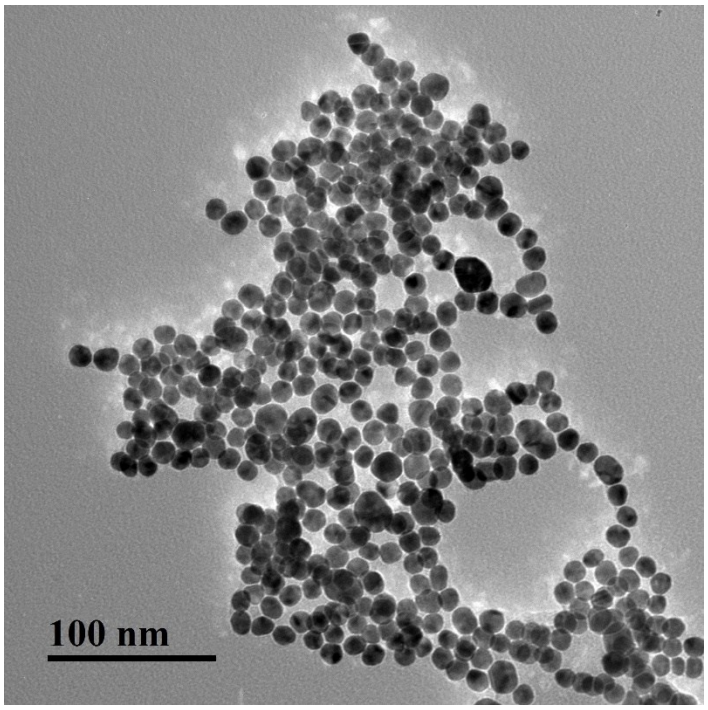

Figure S10. TEM characterization of the L-Cys mediated agminated AuNP-CS.

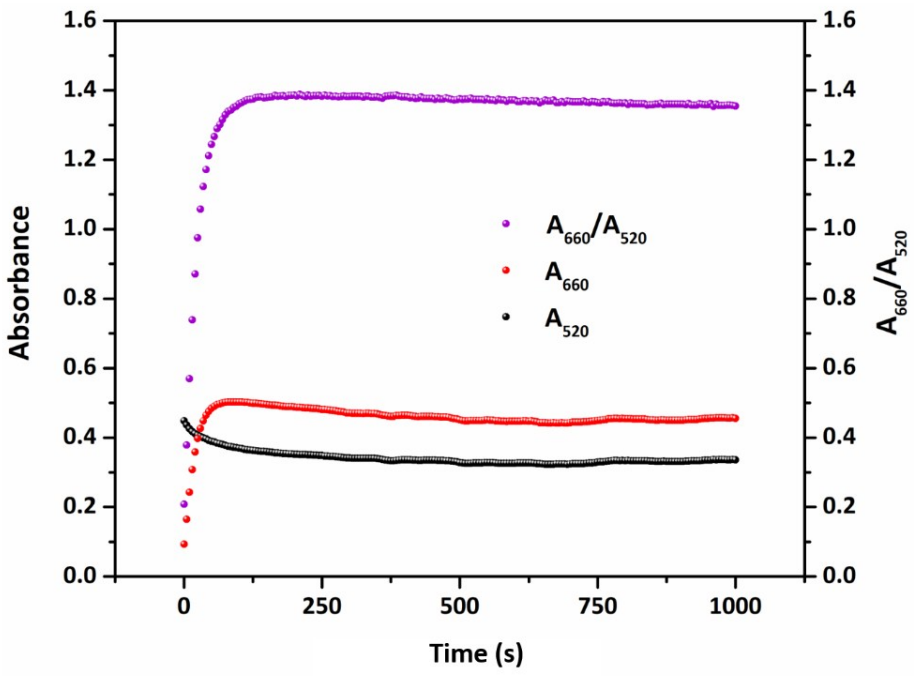

Figure S11. Kinetics for L-Cys mediated aggregation of AuNP-CS.

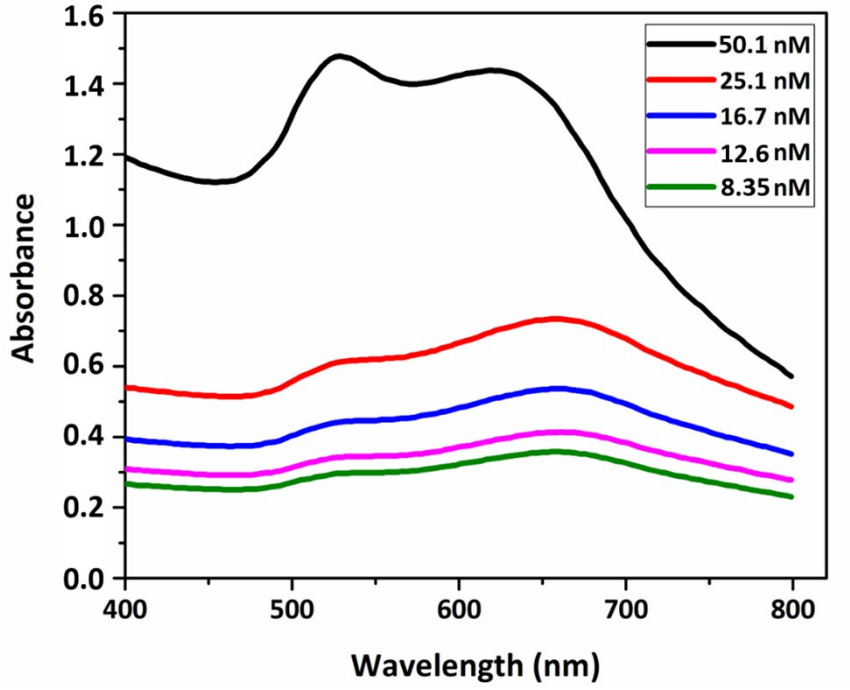

Figure S12. Optimization of the concentration of AuNP-CS.

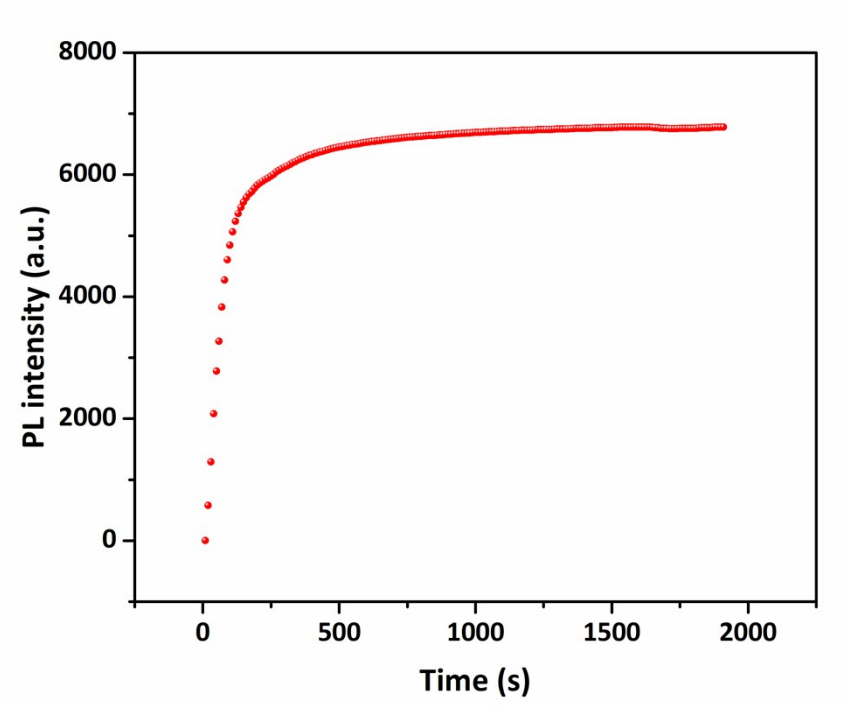

Figure S13. Kinetics of Ins inhibited TR-FRET. The concentration of Ins is 1.5 nM.

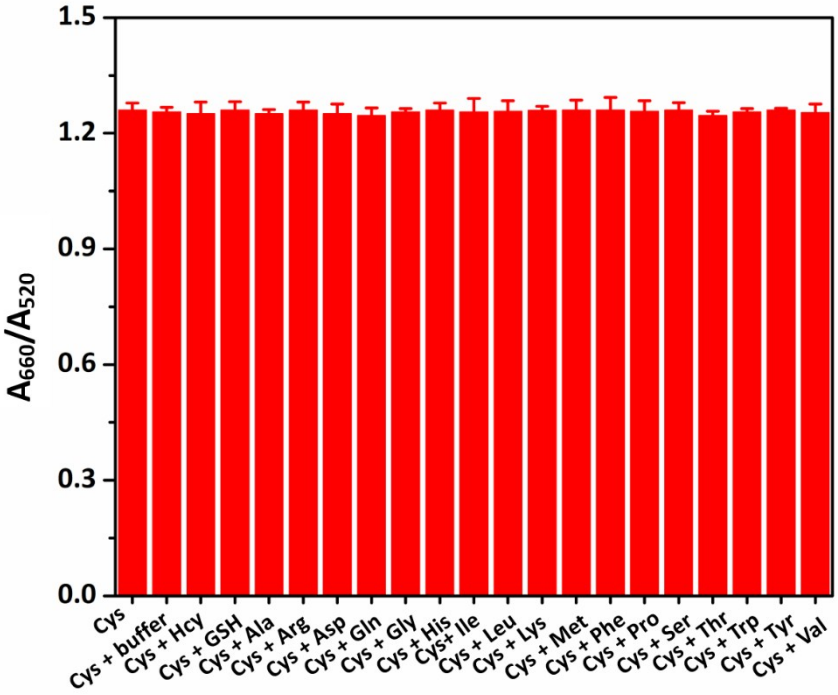

Figure S14. Selectivity of Ratio-Abs based assay for the detection of L-Cys.

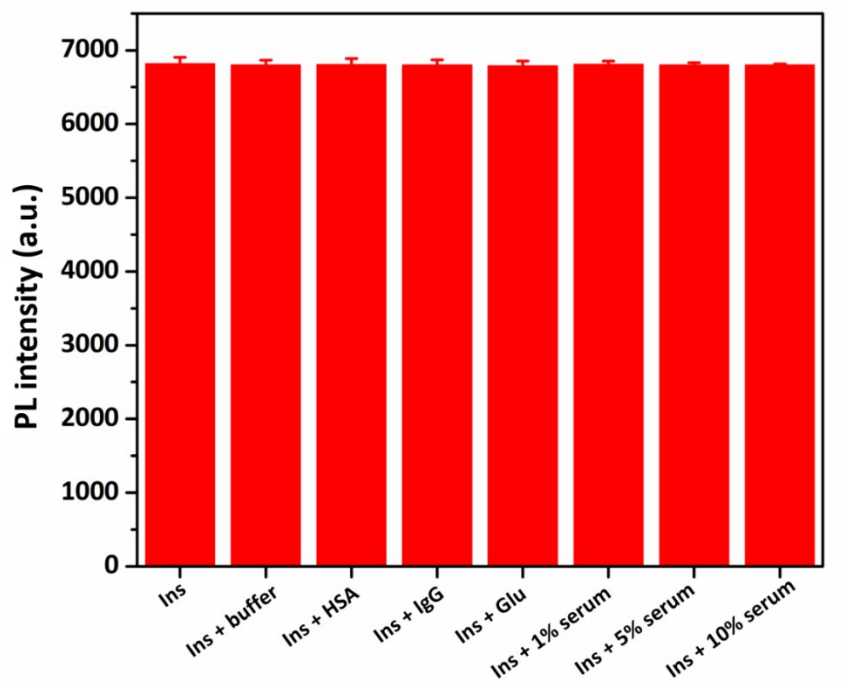

Figure S15. Selectivity of inhibited TR-FRET based assay for the detection of Ins.

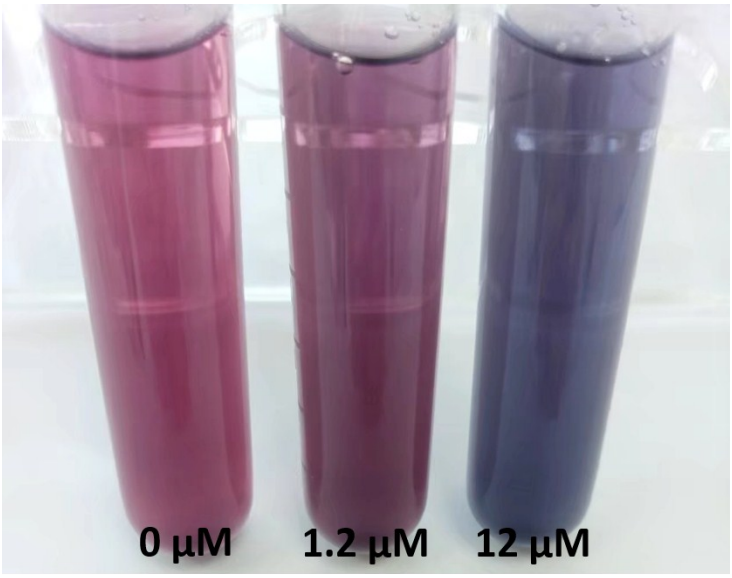

Figure S16. Different concentrations (0, 1.2, and 12 µM) of L-Cys mediated AuNP-CS aggregation.

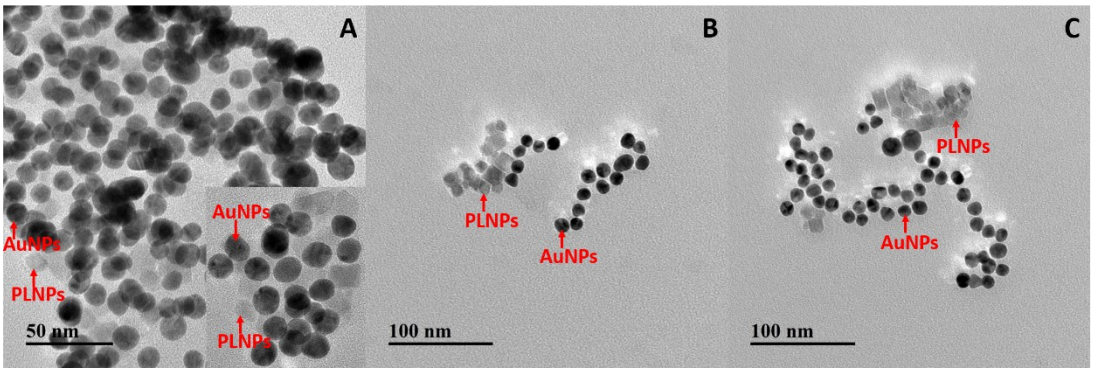

Figure S17. TEM images of detection probes with different concentrations of Ins. (A) Without Ins, (B) and (C) 860 pM of Ins.

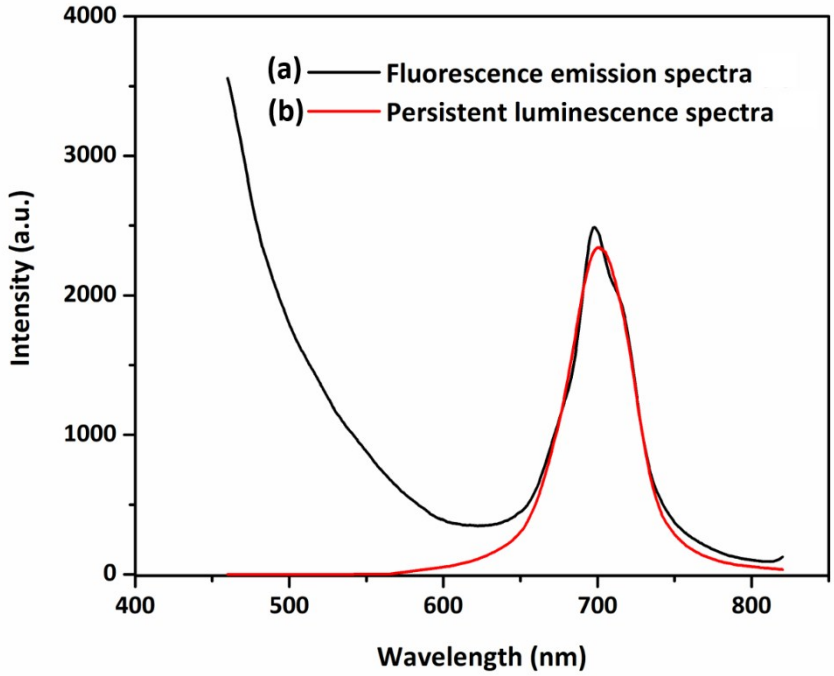

Figure S18. Fluorescence emission spectra and persistent luminescence spectra of PLNP-IBA in serum. (a) In situ excitation; (b) removal of the excitation source and with a delay time of 100 microseconds.

Supplementary Tables S1-S2

Table S1. Performance comparison of different methods for the detection of L-Cys.

Methods	Liner range	Detection limit	Ref.
CDs-Hg^{2+} system	2–20 μM	0.29 μM	[S1]
MoS_2/PDDA-MC based sensor	0.45–155 μM	0.09 μM	[S2]
AuNCs–AuNPs probe	5.0 μM–0.5 mM	3.6 μM	[S3]
A single electrochemical biosensor	1–12 μM	480 nM	[S4]
Eu-GQDs	0.5–50 μM	0.31 μM	[S5]
BFCs based self-powered sensor	0.02–3 μM	10 nM	[S6]
FSN-capped AuNPs	0.2–3.0 μM	0.15 μM	[S7]
The developed method	0.01–5.5 μM	2.2 nM	This work

Table S2. Performance comparison of different methods for the detection of Ins.

Methods	Liner range	Detection limit	Refs
IBA-MMANs	2–1000 ng mL^{-1}	2.0 ng mL^{-1}	[S8]
G-Quadruplex-based detection platform	80 pM–20 nM	80 pM	[S9]
PEC sandwich transducer	0.01– 50 ng mL^{-1}	2.8 pg mL^{-1}	[S10]
Insulin-EMMIPs	0.01–1 nM	3 pM	[S11]
NIR-FRET-based on aptamer	1 pM–2 nM	0.6 pM	[S12]
Aptamer-mediated composite fluorescent probe	4.3–206.4 nM	2.74 nM	[S13]
Impedimetric sensor	1–1000 ng mL^{-1}	70 pg mL^{-1}	[S14]
The developed method	0.012–3.44 nM	2.06 pM	This work

References

1 F. Yan, D. Shi, T. Zheng, K. Yun, X. Zhou and L. Chen, *Sensors Actuators B: Chem.*, 2016, **224**, 926-935.

2 Z. Zheng, Q. Feng, J. Li and C. Wang, *Sens. and Actuators B: Chem.*, 2015, **221**, 1162-1169.

3 X. Xu, J. Qiao, N. Li, L. Qi and S. Zhang, *Anal. Chim. Acta*, 2015, **879**, 97-103.

4 Y. Luo, L. Zhang, W. Liu, Y. Yu and Y. Tian, *Angew. Chem. Int. Ed. Engl.*, 2015, **54**, 14053-14056.

5 L. Lin, X. Song, Y. Chen, M. Rong, Y. Wang, L. Zhao, T. Zhao and X. Chen, *Anal. Chim. Acta*, 2015, **891**, 261-268.

6 C. Hou, S. Fan, Q. Lang and A. Liu, *Anal. Chem.*, 2015, **87**, 3382-3387.

7 Q. Xiao, F. Shang, X. Xu, Q. Li, C. Lu and J. M. Lin, *Biosens. Bioelectron.*, 2011, **30**, 211-215.

8 Y. Xiong, C. Deng, X. Zhang and P. Yang, *ACS Appl. Mater. Interfaces*, 2015, **7**, 8451-8456.

9 M. Wang, W. Wang, T. S. Kang, C. H. Leung and D. L. Ma, *Anal. Chem.*, 2016, **88**, 981-987.

10 R. Wang, H. Ma, Y. Zhang, Q. Wang, Z. Yang, B. Du, D. Wu and Q. Wei, *Biosens. Bioelectron.*, 2017, **96**, 345-350.

11 W. Zhu, L. Xu, C. Zhu, B. Li, H. Xiao, H. Jiang and X. Zhou, *Electrochim. Acta*, 2016, **218**, 91-100.

12 Y. Wang, D. Gao, P. Zhang, P. Gong, C. Chen, G. Gao and L. Cai, *Chem. Commun. (Camb.)*, 2014, **50**, 811-813.

13 J. Yang, Z. Zhang and G. Yan, *Sensors Actuators B: Chem.*, 2018, **255**, 2339-2346.

14 A. K. Yagati, Y. Choi, J. Park, J. W. Choi, H. S. Jun and S. Cho, *Biosens. Bioelectron.*, 2016, **80**, 307-314.